Simple Design Method for a Tuned Viscous Mass Damper Seismic Control System

K. Ikago
Tohoku University, Japan

Y. Sugimura & K. Saito
NTT Facilities Inc., Japan

N. Inoue
Tohoku University, Japan

SUMMARY:
A tuned viscous mass damper (TVMD) using a ball screw mechanism as an apparent mass amplifier has been developed. This device can provide an apparent mass that is large enough to enable effective seismic control.
For a TVMD seismic control system, various design methods based on numerical optimization and spectrum modal analysis have been presented in previous studies. However, these methods require complex-valued eigenvalue problem analysis because multi-degree-of-freedom (MDOF) systems incorporated with TVMDs are nonproportionally damped.
Because practicing structural designers are often unfamiliar with complex-valued eigenvalue analysis and numerical optimization, a simpler design method based on real-valued eigenvalue problem analysis is desirable for a practical structural design.
This paper proposes such a simple design method for MDOF TVMD seismic control systems. A design example illustrates that the present method approximates the seismic response of such systems well.

Keywords: tuned viscous mass damper, seismic control, flywheel, SRSS, CQC

1. INTRODUCTION

Saito *et al*. (2008) developed a seismic control system by connecting a soft spring to a rotary damping tube with inertial mass (Fig. 1.1). This system is called the tuned viscous mass damper (TVMD) system (Ikago, Saito, and Inoue 2012). The basic concept of TVMDs is the same as that of a tuned mass damper (TMD) or a dynamic vibration absorber. Furthermore, its optimal design is obtained using fixed points (Den Hartog 1956) on the resonance curve of a single-degree-of-freedom (SDOF) system incorporated with a TVMD.

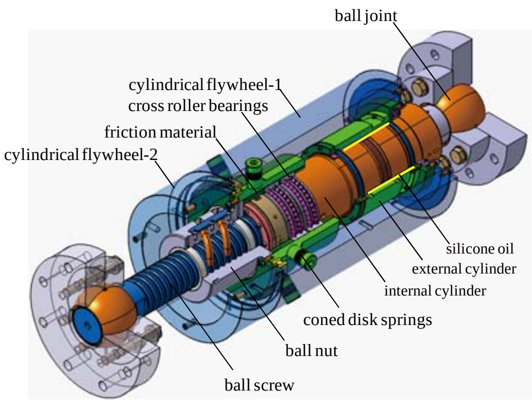

Figure 1.1. Rotary Damping Tube with Inertial Mass

It is known that TMDs for buildings are effective against wind-induced vibrations (McNamara 1979). However, a statistical study on TMD systems with a secondary mass ratio of less than 0.02 showed that it is not necessarily effective against earthquake-induced vibrations (Kaynia, Veneziano, and Biggs 1981).

Hence, a secondary mass that is larger than the effective mass of the primary structure by several percent is required to achieve effective reduction in seismic vibrations. Installing such a large mass in a building is impractical. Nevertheless, a large apparent mass can be easily obtained by a mass amplifying mechanism using a ball screw and a cylindrical flywheel with a small actual mass in the TVMD system (Ikago *et al.* 2011a).

For a multi-degree-of-freedom (MDOF) TVMD seismic control system, design methods based on numerical optimization have already been presented (Ikago *et al.* 2011a, b). However, simpler practical design methods have not yet been proposed.

At the preliminary design stage, it is essential for structural designers to understand the seismic response characteristics of a structure in terms of modal responses. Although complex-valued eigenvalue problem analysis is necessary because seismic control systems with TVMDs are nonproportionally damped, complex modes are not commonly used in practice. Instead, undamped real modes are used.

In this study, a design example is employed to illustrate a simple design method without the need for complex-valued eigenvalue problem analysis and numerical optimization.

2. ANALYSIS MODEL

Figures 2.1. and 2.2. show the TVMD analytical model and a MDOF structure incorporated with TVMDs, respectively. m_i, k_i and c_i are the mass, stiffness, and damping coefficients of the i th story, and m_{ri}, k_{bi} and c_{di} represent the secondary apparent mass, supporting spring stiffness, and damping coefficient of the i th story incorporated with TVMDs.

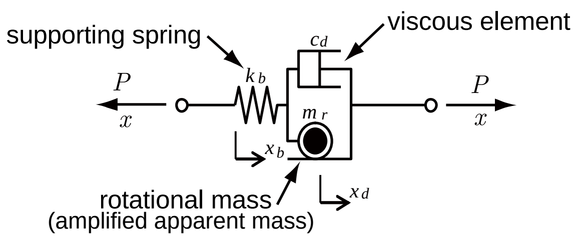

$$P = k_b x_b$$
$$= m_r \ddot{x}_d + c_d \dot{x}_d$$
$$x = x_b + x_d$$

Figure 2.1. TVMD model

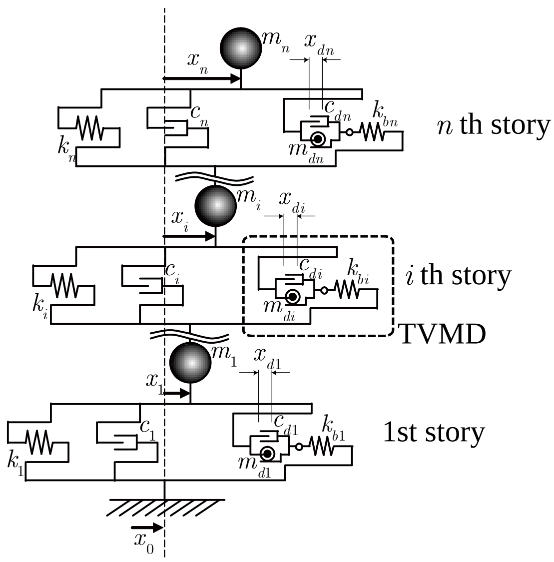

Figure 2.2. Analytical model

When TVMDs are incorporated into a primary structure subjected to seismic ground motion, a component of the interstory motion that is resonant with the secondary vibration system results in amplified motion and substantial energy dissipation in dashpots.

In this study, we use a 10-story benchmark structure S45 model provided in the report on the research and development in the U.S.-Japan cooperative structural testing research program on smart structural systems (BRI and BCJ, 2001) as a seismic control design example. The characteristics of the benchmark structure are listed in Tables 2.1. and 2.2.

An equivalent SDOF structure incorporated with an equivalent TVMD system to estimate modal responses and its analytical model are shown in Fig. 2.3.

Table 2.1. Specifications of the analytical model

story	primary structure		
	mass [t]	stiffness[kN/m]	height[m]
10	399	152790	4
9	399	242600	4
8	399	316920	4
7	399	380260	4
6	399	434360	4
5	399	480140	4
4	399	518110	4
3	399	548620	4
2	399	571920	4
1	399	588180	4

Table 2.2. Undamped fundamental period

Mode	1st	2nd	3rd
period(s)	1.20	0.47	0.29
angular frequency	5.23	13.5	21.5

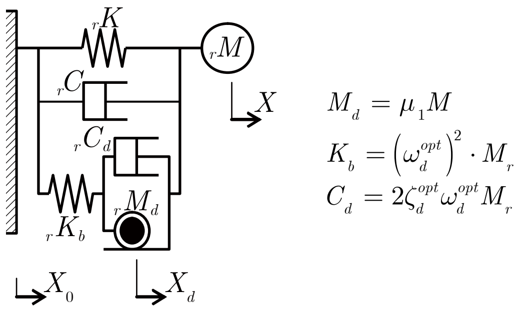

Figure 2.3. Equivalent SDOF structure incorporated with a TVMD

In Fig. 2.3., $_rM$, $_rC$, and $_rK$ are the generalized mass, damping coefficient, and stiffness coefficient for the r th mode of the primary structure, respectively. $_rM_d$, $_rC_d$, and $_rK_d$ are the generalized mass, damping coefficient, and stiffness coefficient for the r th mode of the secondary system, respectively. The ratios of the generalized mass and frequency of the secondary to the primary systems are represented by μ and β, respectively. ζ_d is the ratio of the damping coefficient and critical damping coefficient of the secondary system.

3. EQUATIONS OF MOTION

3.1. Equations of Motion for the Uncontrolled Primary System

The equations of motion for the uncontrolled primary structure are as follows:

$$\mathbf{M}_p \ddot{\boldsymbol{x}}_p + \mathbf{C}_p \dot{\boldsymbol{x}}_p + \mathbf{K}_p \boldsymbol{x}_p = -\mathbf{M}_p \mathbf{1} \ddot{x}_0 , \tag{3.1}$$

where $\boldsymbol{x}_p = \{x_1, x_2, \cdots, x_n\}^T$ is the displacement vector of the primary system relative to the ground, $\mathbf{1} = \{1,1,1,\cdots,1\}^T$ is the influence coefficient vector, $\mathbf{C}_p$ is the inherent damping matrix for the primary structure, and superscript T denotes matrix transpose.

$$\mathbf{M}_p = \begin{bmatrix} m_1 & 0 & \cdots & 0 \\ 0 & m_2 & & \vdots \\ \vdots & & \ddots & \\ & & & 0 \\ 0 & \cdots & 0 & m_n \end{bmatrix}, \mathbf{K}_p = \begin{bmatrix} k_1 + k_2 & -k_2 & \cdots & 0 \\ -k_2 & k_2 + k_3 & -k_3 & \vdots \\ 0 & & \ddots & 0 \\ \vdots & -k_{n-1} & k_{n-1} + k_n & -k_n \\ 0 & \cdots & -k_n & k_n \end{bmatrix}. \tag{3.2}$$

If we assume that $\mathbf{C}_p$ is proportional to the stiffness matrix and the inherent damping ratio for the 1st mode of the primary structure ${}_1\xi$ equals 0.02, then $\mathbf{C}_p$ is given by

$$\mathbf{C}_p = \frac{2\,{}_1\xi}{{}_1\omega_p}\mathbf{K}_p = \frac{0.04}{{}_1\omega_p}\mathbf{K}_p\,, \tag{3.3}$$

where ${}_1\omega_p$ is the lowest fundamental angular frequency of the undamped primary structure.

3.2 Equations of Motion for the MDOF Seismic Control System Incorporated with TVMDs

The equations of motion of a damped n-DOF structure incorporated with one TVMD in each story, i.e., n TVMDs in the entire structure (Fig. 2.2.), are described as follows:

$$\mathbf{M}\ddot{\boldsymbol{x}} + \mathbf{C}\dot{\boldsymbol{x}} + \mathbf{K}\boldsymbol{x} = -\mathbf{M}\mathbf{r}\ddot{x}_0\,, \tag{3.4}$$

where $\boldsymbol{x}$ is a $2n$-dimensional column vector consisting of an n-dimensional displacement vector of the primary system relative to the ground and an n-dimensional deformation vector of each damper in each story. In this study, $n = 10$ and

$$\boldsymbol{x} = \{\boldsymbol{x}_p^T, x_{n+1}, x_{n+2}, \cdots, x_{2n}\}^T\,, \tag{3.5}$$

where $x_{n+i} = x_{di}$ is the displacement of the apparent mass and viscous element of the TVMD installed in the ith story.

The lower half of the influence coefficient vector $\mathbf{r}$ is the n-dimensional zero vector, whereas its upper half is the n-dimensional unit vector. This is because the TVMDs are not activated by ground motion but by the relative displacement in each story:

$$\mathbf{r} = \{1, 1, \cdots, 1, 0, 0, \cdots, 0\}^T\,. \tag{3.6}$$

$\mathbf{M}, \mathbf{C},$ and $\mathbf{K}$ denote the following $2n$-dimensional mass, damping, and stiffness matrices, respectively.

$$\mathbf{M} = \begin{bmatrix} \mathbf{M}_p & \mathbf{O} \\ \mathbf{O} & \mathbf{M}_r \end{bmatrix},\ \mathbf{C} = \begin{bmatrix} \mathbf{C}_p & \mathbf{O} \\ \mathbf{O} & \mathbf{C}_d \end{bmatrix},\ \mathbf{K} = \begin{bmatrix} \mathbf{K}_p + \mathbf{K}_{b11} & \mathbf{K}_{b12} \\ \mathbf{K}_{b21} & \mathbf{K}_{b22} \end{bmatrix}, \tag{3.7}$$

where

$$\mathbf{M}_r = \begin{bmatrix} m_{d1} & 0 & \cdots & & 0 \\ 0 & m_{d2} & & & \vdots \\ \vdots & & \ddots & & \\ & & & & 0 \\ 0 & \cdots & & 0 & m_{dn} \end{bmatrix},\ \mathbf{C}_d = \begin{bmatrix} c_{d1} & 0 & \cdots & & 0 \\ 0 & c_{d2} & & & \vdots \\ \vdots & & \ddots & & \\ & & & & 0 \\ 0 & \cdots & & 0 & c_{dn} \end{bmatrix}, \tag{3.8}$$

$$\mathbf{K}_{b11} = \begin{bmatrix} k_{b1} + k_{b2} & -k_{b2} & \cdots & 0 \\ -k_{b2} & k_{b2} + k_{b3} & -k_{b3} & \vdots \\ 0 & & \ddots & 0 \\ \vdots & -k_{b,n-1} & k_{b,n-1} + k_{bn} & -k_{bn} \\ 0 & \cdots & -k_{bn} & k_{bn} \end{bmatrix}, \mathbf{K}_{b21} = \mathbf{K}_{b12}^T \tag{3.9}$$

$$\mathbf{K}_{b12}=\begin{bmatrix}-k_{b1} & k_{b2} & \cdots & & 0\\ 0 & -k_{b2} & k_{b3} & & \vdots\\ & & \ddots & \ddots & 0\\ \vdots & & & -k_{b,n-1} & k_{bn}\\ 0 & \cdots & & 0 & -k_{bn}\end{bmatrix},\ \mathbf{K}_{b22}=\begin{bmatrix}k_{b1} & 0 & \cdots & & 0\\ 0 & k_{b2} & & & \vdots\\ \vdots & & \ddots & & \\ & & & & 0\\ 0 & \cdots & & 0 & k_{bn}\end{bmatrix}. \tag{3.10}$$

4. EIGENVALUE PROBLEM ANALYSES

4.1 Eigenvalue problem analysis of the undamped primary structure

The characteristic equation derived from the eigenvalue problem for the undamped primary structure is

$$\left|\mathbf{K}_p-\Omega_p\mathbf{M}_p\right|=0. \tag{4.1}$$

Let ${}_r\Omega_p$ and ${}_r\boldsymbol{\phi}_p$ denote the r th eigenvalue and eigenvector derived from Eq.(4.1) respectively. Then, the r th undamped fundamental angular frequency ${}_r\omega_p$ that equals the square root of the r th eigenvalue is given by the following:

$${}_r\omega_p=\sqrt{{}_r\Omega_p}\ . \tag{4.2}$$

4.2. Eigenvalue problem analysis of the controlled structure

Because the MDOF seismic control system with TVMDs is nonproportionally damped, it is intrinsically required to conduct complex-valued eigenvalue problem analysis to obtain its exact eigenvalues and damping ratios. To this end, Eq. (3.4) is converted into the following $4n$ first-order matrix equation:

$$\mathbf{A}\dot{\boldsymbol{y}}+\mathbf{B}\boldsymbol{y}=-\mathbf{A}\boldsymbol{w}\ddot{x}_g(t), \tag{4.3}$$

where

$$\mathbf{A}=\begin{bmatrix}\mathbf{O} & \mathbf{M}\\ \mathbf{M} & \mathbf{C}\end{bmatrix},\mathbf{B}=\begin{bmatrix}-\mathbf{M} & \mathbf{O}\\ \mathbf{O} & \mathbf{K}\end{bmatrix},\boldsymbol{w}=\begin{Bmatrix}\mathbf{r}\\ \mathbf{O}\end{Bmatrix},\boldsymbol{y}=\begin{Bmatrix}\dot{\boldsymbol{x}}\\ \boldsymbol{x}\end{Bmatrix}. \tag{4.4}$$

The eigenvalue problem in Eq. (4.3) can be expressed as follows:

$$\mathbf{B}\,{}_i\hat{\boldsymbol{\phi}}_C=-{}_i\lambda_C\mathbf{A}\,{}_i\hat{\boldsymbol{\phi}}_C\,. \tag{4.5}$$

If we assume that this seismic control system is underdamped, the eigenvalues and eigenvectors given by Eq. (4.5) are $2n$ complex conjugate pairs.

Here, we express the r th pairs of eigenvalues and eigenvectors as ${}_{2r-1}\lambda_C,{}_{2r}\lambda_C$ and ${}_{2r-1}\hat{\boldsymbol{\phi}}_C,{}_{2r}\hat{\boldsymbol{\phi}}_C$, respectively.
The r th fundamental angular frequency ${}_r\omega_C$ and the corresponding damping ratio ${}_r\xi_C$ can be obtained as follows:

$${}_r\omega_C=|{}_{2r-1}\lambda_C|=|{}_{2r}\lambda_C|,\quad {}_r\xi_C=-\frac{\mathrm{Re}[{}_{2r-1}\lambda_C]}{|{}_{2r-1}\lambda_C|}=-\frac{\mathrm{Re}[{}_{2j}\lambda_C]}{|{}_{2j}\lambda_C|}\ . \tag{4.6}$$

4.3. Approximated Eigenvalue Problem Analysis of the MDOF TVMD System Using the Undamped System

In Eq. (3.4), the effect of the damping matrix is neglected to avoid complex-valued eigenvalue problem analysis. Then, the characteristic equation of the MDOF TVMD system reduces to

$$\left|\mathbf{K}-\Omega\mathbf{M}\right|=0\,. \tag{4.7}$$

Let ${}_r\Omega$ and ${}_r\phi_R$ denote the r th eigenvalue and eigenvector derived from Eq.(4.7), respectively. The r th approximated fundamental angular frequency ${}_r\omega_R$ equals the square root of the r th eigenvalue:

$${}_r\omega_R=\sqrt{{}_r\Omega}\,. \tag{4.8}$$

It is well known that a good approximation of the r th modal damping ratio ${}_r\xi_R$ is given by

$${}_r\xi_R=\frac{{}_r\phi_R^T\mathbf{C}\,{}_r\phi_R}{2\,{}_r\omega_R\,{}_r\phi_R^T\mathbf{M}\,{}_r\phi_R}\,, \tag{4.9}$$

if the vibration system is slightly damped.

5. ANALYSIS EXAMPLE

The damping effect of the TVMD system is closely related to the effective modal mass ratio. The generalized modal mass for the undamped primary structure is

$${}_1M={}_1\boldsymbol{\phi}_p^T\mathbf{M}_p\,{}_1\boldsymbol{\phi}_p=\sum_{j=1}^{n}m_j\,{}_1\phi_{p,j}^2\,. \tag{5.1}$$

Because the TVMD system is activated by the interstory displacements of the primary structure, the effective modal mass of the additional vibration system tuned to the first mode is expressed as follows:

$${}_1M_d=m_{d,1}\,{}_1\phi_{p,1}^2+\sum_{j=2}^{n}m_{d,j}\left({}_1\phi_{p,j}-{}_1\phi_{p,j-1}\right)^2\,. \tag{5.2}$$

Thus, the effective mass ratio is given by ${}_1\mu={}_1M_d\,/\,{}_1M$. In this study, an additional mass ratio of 0.1 is specified, and the distribution of the additional masses is set such that it is proportional to that of story stiffness:

$$m_{d,i}=\alpha k_i\,. \tag{5.3}$$

Substituting Eq. (5.3) into Eq. (5.2) yields

$${}_1M_d=\alpha\left[k_1\,{}_1\phi_{p,1}^2+\sum_{j=2}^{n}k_j\left({}_1\phi_{p,j}-{}_1\phi_{p,j-1}\right)^2\right]=\alpha\cdot{}_1\boldsymbol{\phi}_p^T\mathbf{K}_p\,{}_1\boldsymbol{\phi}_p\,. \tag{5.4}$$

Thus,

$$\alpha=\frac{{}_1M_d}{{}_1\boldsymbol{\phi}_p^T\mathbf{K}_p\,{}_1\boldsymbol{\phi}_p}=\frac{\mu\,{}_1M}{{}_1\boldsymbol{\phi}_p^T\mathbf{K}_p\,{}_1\boldsymbol{\phi}_p}=\frac{\mu\cdot{}_1\boldsymbol{\phi}_p^T\mathbf{M}_p\,{}_1\boldsymbol{\phi}_p}{{}_1\boldsymbol{\phi}_p^T\mathbf{K}_p\,{}_1\boldsymbol{\phi}_p}=\frac{\mu}{{}_1\Omega}\,. \tag{5.5}$$

For the equivalent SDOF system incorporated with TVMDs, the optimal angular frequency ω_r^{opt} and damping ratio ζ_d^{opt} for the specified mass ratio μ are obtained by the fixed point method (Saito *et al*. 2008):

$$k_{b,i} = \left(\omega_d^{opt}\right)^2 m_{d,i}, \quad c_{d,i} = 2\zeta_d^{opt}\omega_d^{opt} m_{d,i}\,, \tag{5.6}$$

where

$$\omega_d^{opt} = \frac{1-\sqrt{1-4\mu}}{2\mu}\cdot {}_1\omega_p, \quad \zeta_d^{opt} = \frac{\sqrt{3(1-\sqrt{1-4\mu})}}{4}\,. \tag{5.7}$$

The calculated values are shown in Table 5.1.

Although each secondary mass is larger than each primary mass in the corresponding story, as shown in Table 5.1., the actual masses required are reduced to several thousandths by the mass amplifying mechanism.

Here, we compare the fundamental angular frequencies, damping ratios, and participation vectors obtained by the following three methods:

Method A. The eigenvalue problem analysis of the undamped primary system. (the real-valued analysis shown in section 4.1.)
Method B. The complex-valued eigenvalue problem analysis of the TVMD seismic control system. (the complex-valued analysis shown in section 4.2.)
Method C. The eigenvalue problem analysis of the TVMD seismic control system ignoring the damping matrix. (the real-valued analysis shown in section 4.3)

Table 5.2. compares the fundamental angular frequencies and damping ratios obtained by the three methods. The 1st mode of the uncontrolled primary system is split into 11 modes by adding the 10-DOF secondary system. The fundamental angular frequencies of the 1st to 11th modes of the TVMD system obtained by Methods B and C are close to each other. They are also close to the 1st fundamental angular frequency of the uncontrolled primary system obtained by Method A. The damping ratios of the 2nd and 3rd modes of the uncontrolled primary system are almost unchanged by the addition of TVMDs, whereas those of the 1st to 11th modes of the TVMD system are substantially increased. This means that the TVMD seismic control system can increase the damping ratio of the specified mode, and it almost never changes those of the other modes.

The damping ratios of the 2nd to 10th conjugate pair modes are almost identical to the local damping ratio of the device $\zeta_d^{opt} = \sqrt{3(1-\sqrt{1-4\mu})}\,/\,4 = 0.206$. This is because only the secondary masses, as observed in Fig. 5.1(b), are activated in these modes and are independent of the primary responses.
As shown in Table 5.2., the modal damping ratios obtained from Eq. (4.9) (Method C) correspond well with those obtained from complex-valued eigenvalue problem analysis (Method B).
Figure 5.1. compares the modal participation vectors obtained by Methods A, B, and C. The modal participation vectors obtained by Method C give a good approximation of the real parts of the complex valued modal participation vectors obtained by Method B.

Although complex-valued eigenvalue problem analysis (Method B) is intrinsically inevitable in the spectrum modal analysis of the TVMD seismic control system, the above comparisons of the three methods suggest that Method C may also give a good seismic response estimate.

Table 5.1. Specifications of the TVMD system

story	$m_{d,i}$ [t]	$k_{b,i}$ [kN/m]	$c_{d,i}$ [kNs/m]
10	558	19407	1353
9	885	30814	2148
8	1157	40254	2805
7	1388	48299	3366
6	1585	55171	3845
5	1752	60986	4250
4	1891	65809	4586
3	2002	69684	4857
2	2087	72643	5063
1	2147	74709	5207

Table 5.2. Comparison of angular frequencies and damping ratios

mode	Uncontrolled Method A.		mode	TVMD system Method B.		TVMD system Method C.	
	angular frequency	damping ratio		angular frequency	damping ratio	angular frequency	damping ratio
1	5.23	0.02	1	4.79	0.122	4.65	0.121
			2	5.50	0.218	5.50	0.218
			3	5.54	0.220	5.54	0.220
			4	5.55	0.220	5.55	0.220
			5	5.55	0.220	5.55	0.220
			6	5.55	0.221	5.55	0.221
			7	5.55	0.221	5.55	0.221
			8	5.55	0.221	5.55	0.221
			9	5.55	0.221	5.55	0.221
			10	5.55	0.221	5.56	0.221
			11	6.44	0.114	6.64	0.114
2	13.5	0.052	12	14.5	0.049	14.5	0.049
3	21.5	0.082	13	23.0	0.077	23.0	0.077

Here, we propose the following approximation for the maximum interstory drifts $\{\delta_i\}$ and damper forces $\{f_{d,i}\}$:

$$\delta_i = \sqrt{\sum_{k=1,n+1} \left\{ S_D\left({}_k\omega_R; {}_k\xi_R\right) {}_k\nu \left({}_k\phi_{R,i} - {}_k\phi_{R,i-1} \right) \right\}^2 + \sum_{k=n+2}^{2n} \left\{ S_D\left({}_k\omega_R; {}_k\xi_R\right) {}_k\nu \left({}_k\phi_{R,i} - {}_k\phi_{R,i-1} \right) \right\}^2} \quad ,(5.8)$$

$$f_{d,i} = k_{b,i} \sqrt{\sum_{k=1,n+1} \left\{ S_D\left({}_k\omega_R; {}_k\xi_R\right) {}_k\nu\, {}_k\phi_{b,i} \right\}^2 + \sum_{k=n+2}^{2n} \left\{ S_D\left({}_k\omega_R; {}_k\xi_R\right) {}_k\nu\, {}_k\phi_{b,i} \right\}^2} \quad , \tag{5.9}$$

where ${}_k\nu$ is the modal participation factor for the kth mode. ${}_k\phi_{b,i}$ is the displacement of the damper supporting spring in the ith story and is given by subtracting the damper displacement ${}_k\phi_{i+n}$ from the interstory drift:

$${}_k\phi_{b,i} = {}_k\phi_i - {}_k\phi_{i-1} - {}_k\phi_{i+n} \,. \tag{5.10}$$

Obviously, Eqs. (5.8) and (5.9) are based on the square root of the sum of the squares method. However, the 2nd to nth modal component are eliminated because they are insignificant.

Here, we compare the seismic response estimation methods by using ten synthesized ground motions. The acceleration response spectra of the ground motions are compatible with the target spectrum specified by the building standard law of Japan, whose magnitudes are doubled considering the amplification by the surface ground in this study. The ground motions have random phase angles that are different from each other. The acceleration response spectra of the ground motions are shown in Fig. 5.2.

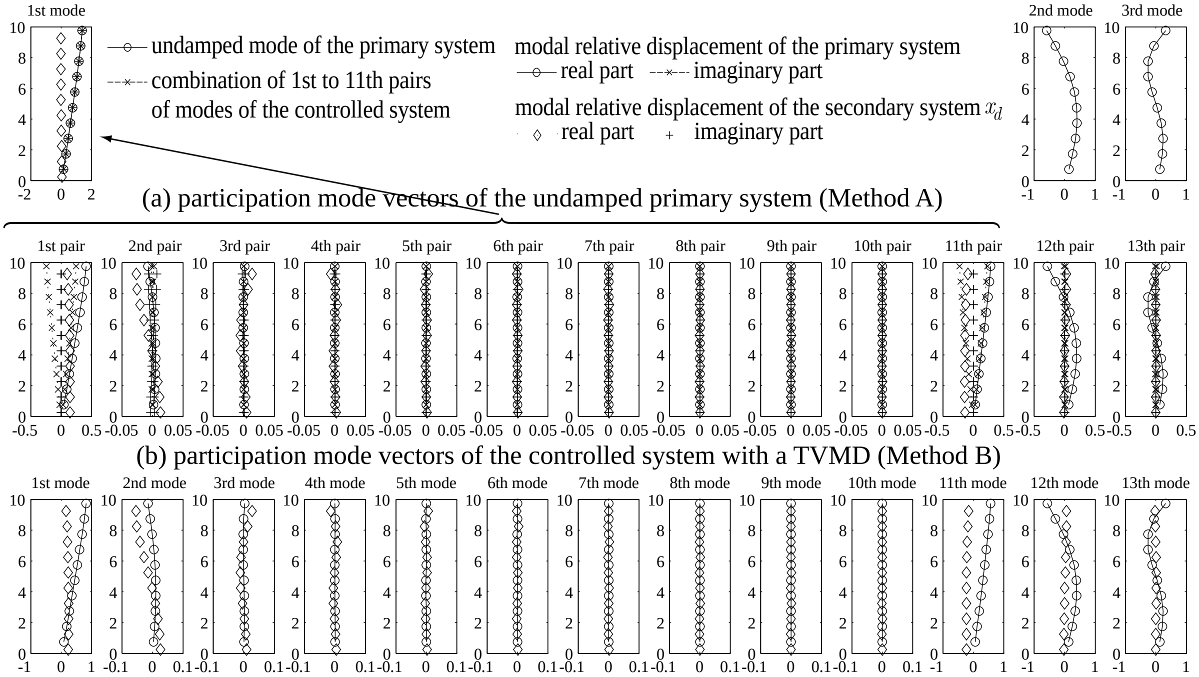

Figure 5.1. Comparison of participation mode vectors

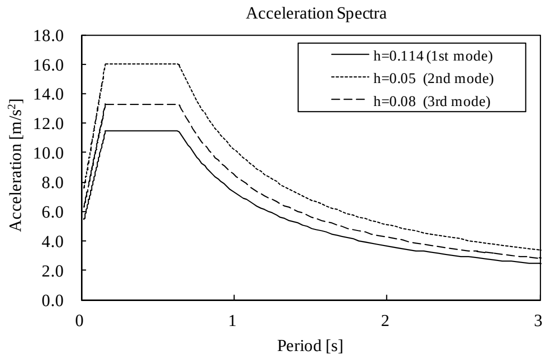

Figure 5.2. Response spectra of the input ground motion

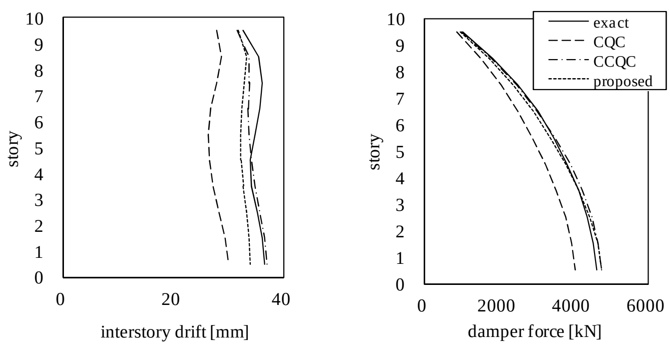

Figure 5.3. Comparison of seismic response estimation

Figure 5.3. compares the average maximum responses obtained from the time history analyses using ten ground motions based on Newmark's β method, the complex complete quadratic combination

method (Yang and Sarkani 1990), the complete quadratic combination (CQC) method (Wilson, Der Kiureghian, and Bayo 1981), and the proposed method. As shown in Fig. 5.3., the proposed method gives a good approximation in practical terms, whereas the CQC method underestimates the response. Although further investigation is still needed with respect to various secondary mass distribution patterns, the basic modal response characteristics of an MDOF system incorporated with TVMDs are elucidated with the proposed method. This simple seismic response estimation method is based on real-valued eigenvalue problem analysis and is suitable for practical structural design.

6. CONCLUSIONS

In this paper, it is shown that a TVMD seismic control system can specify the modal damping ratio of the tuning mode, and the eigenvalues and damping ratios of the other modes are almost never changed from the uncontrolled system. Therefore, seismic control design using TVMDs can be conducted on the basis of spectrum modal analysis. The approximate eigenvalues, modal damping ratios, and mode vectors are obtained from real-valued eigenvalue problem analysis, with which structural designers are familiar, by ignoring the damping matrix of the TVMD seismic control system. An analysis example illustrated that the proposed seismic response estimation method approximated the seismic response quite well in practical terms.

REFERENCES

Den Hartog J. P., (1956) Mechanical Vibrations (4th edn), Dover: New York.

Ikago K., Sugimura Y., Saito K., Inoue N. (2010) Optimum Seismic Response Control of Multiple Degree of Freedom Structures using Tuned Viscous Mass Dampers, Proceedings of the Tenth International Conference on Computational Structures Technology, Valencia, Spain: Paper 164. DOI:10.4203/ccp.93.164.

Ikago K., Sugimura Y., Saito K., Inoue N. (2011a) Seismic displacement control of multiple-degree-of-freedom structures using tuned viscous mass dampers, Proceedings of the 8th International Conference on Structural Dynamics, EURODYN, Leuven, Belgium, 4-6 July 2011, pp. 1800-1807. (ISBN 978-90-760-1931-4)

Ikago K., Saito K., Inoue N. (2011b) Optimum Multi-modal Seismic Control Design of High-rise Buildings using Tuned Viscous Mass Dampers, Proceedings of the 13th International Conference on Civil, Structural and Environmental Engineering Computing, Chania, Crete, Greece, 2011.9, Paper 170, DOI:10.4203/ccp.96.170.

Ikago K., Saito K., Inoue N. (2012) Seismic control of single-degree-of-freedom structure using tuned viscous mass damper, Earthquake Engineering & Structural Dynamics, Vol. 41, No. 3, pp. 453-474, March 2012. DOI:10.1002/eqe.1138.

Kaynia A. M., Veneziano D., Biggs J. (1981) Seismic effectiveness of tuned mass dampers, Journal of the Structural Division ASCE, Vol. 107, No. 9, pp. 1465-1484.

McNamara RJ. (1979) Tuned mass dampers for buildings, Journal of Structural Engineering ASCE, Vol. 103, No. 9, pp. 1785-1798.

Saito K., Sugimura Y., Nakaminami S., Kida H., Inoue N. (2008) Vibration Tests of 1-story Response Control System Using Inertial Mass and Optimized Soft Spring and Viscous Element, Proceedings of the 14th World Conference on Earthquake Engineering, Beijing, China, Paper ID 12-01-0128.

Building Research Institute (BRI) and the Building Center of Japan (BCJ) (2001), Annual report on the research and development in the U.S.-Japan corporative structural testing research program on smart structural systems (in Japanese).

Wilson E. L., Der Kiureghian A., Bayo E. P. (1981) A replacement for the srss method in seismic analysis.

Yang J. N., Sarkani S. (1990) A response spectrum approach for seismic analysis of non-classically damped structures, Engineering Structures, Vol. 12, pp. 173-184.

ACKNOWLEDGMENTS

This work was supported by a Grant-in-Aid for Scientific Research (B) No. 21360260 provided by the Japan Society for the Promotion of Science (JSPS) and a research grant provided by the Japan Iron and Steel Federation (JISF).